

## Electronic structure as a function of doping in $\text{YBa}_2\text{Cu}_3\text{O}_x$ ( $6.2 \leq x \leq 6.9$ ) studied by angle-resolved photoemission

Rong Liu, B. W. Veal, C. Gu, A. P. Paulikas, and P. Kostic  
*Materials Science Division, Argonne National Laboratory, Argonne, Illinois 60439*

C. G. Olson

*Ames Laboratory, Ames, Iowa 50011*

(Received 17 January 1995)

We report angle-resolved photoemission studies on  $\text{YBa}_2\text{Cu}_3\text{O}_x$  with oxygen stoichiometry varied in the range  $6.2 \leq x \leq 6.9$ . The distinct 1-eV peak, observed with  $h\nu=24$  eV at the  $X(Y)$  point(s), shifts monotonically toward higher binding energies (as much as 0.20 eV) as oxygen stoichiometry is reduced from  $x=6.9$  to 6.3. The direction and the magnitude of the shift are consistent with a simple rigid-band filling picture. However, another distinct peak observed at the  $X(Y)$  point(s), but with energy very close to  $E_F$ , remains at nearly the same energy when the oxygen stoichiometry is varied from 6.9 to 6.4. This behavior is not consistent with a rigid-band picture. The intensities of the 1-eV peak and the peak at  $E_F$  are significantly attenuated when the material becomes insulating.

A common feature of the high- $T_c$  copper oxide superconductors is that electrical conductivity can be controlled by varying doping levels through ion substitution or oxygen stoichiometry variation. A range of phases, including high- $T_c$  superconductors, nonsuperconducting (overdoped) metals, and antiferromagnetic insulators can be obtained. For the insulating phases, a band theory description is not appropriate since it predicts metallic behavior. Apparently, the electronic structure in the insulating phases is governed by strong electron-electron correlations which are not adequately treated in band theory. The importance of electron correlation in the superconducting phases is still a subject of controversy. High-resolution angle-resolved photoemission studies on  $\text{YBa}_2\text{Cu}_3\text{O}_{7-\delta}$  (Refs. 1–5) and  $\text{Bi}_2\text{Sr}_2\text{CaCu}_2\text{O}_8$  (Refs. 6 and 7) report observations of Fermi surfaces that are consistent with the results predicted by band theory. These observations suggest that the Fermi-surface dimensions obey Luttinger's theorem and that the electronic structure can be described with Fermi-liquid theory. However, it was pointed out that a non-Fermi-liquid theory can also have a Fermi surface that obeys Luttinger's theorem.<sup>8</sup> An important question is, how does the electronic structure evolve from an antiferromagnetic insulator to a superconductor as the doping level is varied? Photoelectron spectroscopy has been extensively used to address this issue and diverse views were presented.<sup>2–4,9–12</sup> Based on angle-integrated photoemission studies of optimally doped and undoped  $\text{Nd}_{2-x}\text{Ce}_x\text{CuO}_{4-y}$  and  $\text{La}_{2-x}\text{Sr}_x\text{CuO}_4$ , Allen *et al.*<sup>9</sup> suggested that the Fermi level lies at nearly the same energy for both electron and hole doping, in new states that fall in the insulating gap at zero doping. Shen *et al.*<sup>10</sup> studied  $\text{Bi}_2\text{Sr}_2\text{CaCu}_2\text{O}_{8+\delta}$  with a small variation of  $\delta$ . They reported observation of a shift in the chemical potential of 0.15 to 0.2 eV. They concluded that a rigid band

filling picture can describe the behavior in the high-doping regime.

In this paper, we report angle-resolved photoemission (ARPES) studies of  $\text{YBa}_2\text{Cu}_3\text{O}_x$  (YBCO) with oxygen stoichiometry varied in the range  $6.2 \leq x \leq 6.9$ .  $\text{YBa}_2\text{Cu}_3\text{O}_x$  is an excellent system for the study of doping behavior. High quality single crystals with precisely controlled oxygen stoichiometries can be readily prepared. The material has maximum  $T_c$  (92 K) near the maximum oxygen stoichiometry ( $x \sim 6.9$ ).<sup>3</sup> (Note that the material can be slightly overdoped to produce a weak maximum in  $T_c$ .) When oxygen is reduced from  $x=6.9$ ,  $T_c$  monotonically decreases, showing two "plateaus," one near  $x=6.9$  and another near  $x=6.5$ . (Note that this description is traditional; neither feature actually defines a plateau.) A metal (superconducting)-insulator (nonsuperconducting) transition occurs near  $x=6.38$ . We carried out ARPES studies on a series of samples with different oxygen stoichiometries representing different regions in the phase diagram. In our previous papers,<sup>2,3</sup> we examined the electronic structure in narrow energy windows near the Fermi level. In this paper, we shall place more emphasis on the broad valence band.

ARPES data were taken on single crystals of typical dimensions  $1 \times 1 \times 0.1$  mm<sup>3</sup> grown in gold crucibles using a self-flux technique.<sup>13</sup> To obtain the oxygen stoichiometry  $x \geq 6.9$ , samples were heated in  $\text{O}_2$  for six days at 480 °C followed by a four-day treatment at 420 °C and a furnace cool to room temperature. Oxygen stoichiometries  $x < 6.9$  were normally fixed by quenching from 520 °C after equilibrating (for at least 48 h) in a controlled oxygen-nitrogen atmosphere.<sup>14</sup> After quenching to liquid nitrogen, samples were aged at room temperature for at least one week to achieve a stable vacancy-ordered condition.<sup>14</sup> ARPES measurements were made on the Ames-Montana ERG-Seya beamline<sup>15</sup> at the Synchrotron Radi-

ation Center at Stoughton, Wisconsin. Photoelectrons were energy analyzed using a 50-mm-radius hemispherical analyzer mounted on a goniometer. The angular resolution of the analyzer is  $2^\circ$ . For the spectra shown in this paper, the energy resolution varies between 20 and 100 meV. Before mounting in the sample chamber, sample orientations were determined by Laue x-ray diffraction. Samples were cleaved *in situ* in a vacuum better than  $4 \times 10^{-11}$  Torr with the sample temperature at about 20 K. The cleaved surfaces contain the  $a$ - $b$  plane. Since twinned samples were used,  $\Gamma$ - $X$  and  $\Gamma$ - $Y$  are indistinguishable in these experiments. All samples were mounted with the  $a$  ( $b$ ) axes in the horizontal direction. Because spectral features and their intensities are highly dependent on the measurement conditions (photon energy, photon polarization),<sup>1,16</sup> it is important to compare spectra measured under the same conditions when monitoring spectral changes as a function of oxygen stoichiometry.

Figure 1 shows a set of energy distribution curves (EDC's) measured on a fully oxygenated sample ( $x=6.9$ ). The analyzer angle is varied so that the corresponding  $k$  vector is scanned along the  $\Gamma$ - $X$  ( $Y$ ) symmetry line(s) as indicated by the solid dots in the inset. (There is a one-to-one correspondence between the EDC's and the dots shown in the inset.) Photons of energy  $h\nu=24$  eV were

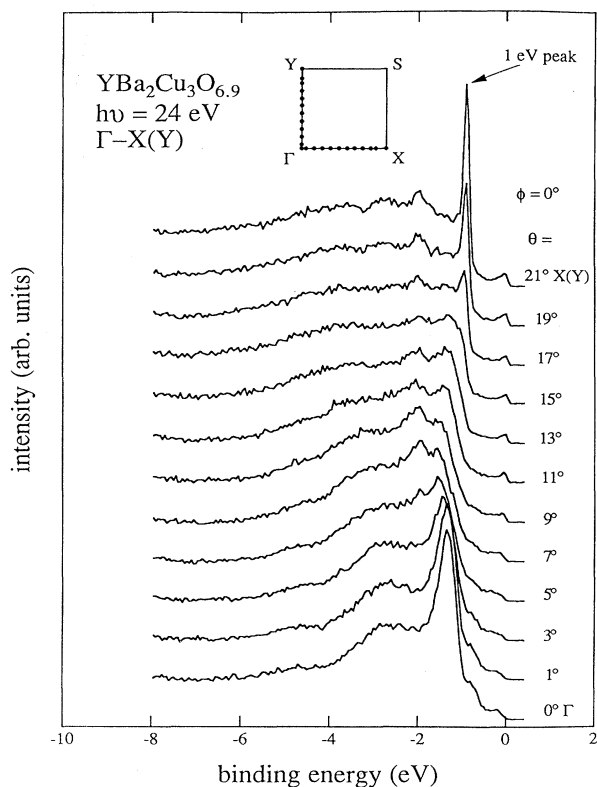


FIG. 1. Energy distribution curves (EDC's) measured on  $\text{YBa}_2\text{Cu}_3\text{O}_{6.9}$ , for  $k$  points along  $\Gamma$ - $X$  ( $Y$ ), using  $h\nu=24$  eV. The photoelectron emission angles ( $\theta$  and  $\phi$ ) relative to the surface normal are marked next to each curve. The corresponding  $k$  points are marked as dots in the Brillouin zone in the inset.

used. The valence band displays distinct and dispersive features. At the  $\Gamma$  point ( $\theta=0^\circ$ ), a prominent peak appears at 1.3 eV below  $E_F$ . As  $k$  is moved away from the  $\Gamma$  point toward the  $X$  ( $Y$ ) point(s), this peak disperses slightly toward higher binding energies. At  $\theta=7^\circ$ , this peak clearly splits into two peaks. As  $k$  is further scanned toward the  $X$  ( $Y$ ) point(s), the peak at the lower binding energy side disperses toward  $E_F$ , while the peak at the higher binding energy side does not show much dispersion. As  $X$  ( $Y$ ) point(s) are approached, the lower binding energy peak becomes extremely sharp. This peak has its lowest binding energy at the  $X$  ( $Y$ ) symmetry point(s). For this fully oxygenated sample, this binding energy is 0.09 eV. In the following, we shall examine the behavior of this peak in more detail. Since this peak is approximately 1 eV below  $E_F$ , we shall call this peak the 1-eV peak for convenience.

The 1-eV peak was observed by Tobin *et al.* at both the  $X$  and the  $Y$  points using twin-free samples,<sup>1</sup> which suggests that this feature is unlikely to be associated with the Cu-O chains but could be associated with the  $\text{CuO}_2$  planes. We also note that sharp spectral features are observed between 1 and 2 eV binding energies at all symmetry points of the Brillouin zone, namely, the  $X$ ,  $Y$ ,  $\Gamma$ , and  $S$  points.<sup>1</sup> The intensities of these features are found to be highly dependent on the photon energy and the relative orientations of the sample crystallographic axes and the photon polarization,<sup>1,16</sup> apparently a manifestation of matrix element effects. The distinct features disperse symmetrically around the symmetry points in the Brillouin zone, which indicates that these states are a direct consequence of the crystallographic periodicity of the material. Some studies have suggested that the 1-eV peak at the  $X$  and  $Y$  points might be attributable to a surface state.<sup>17,18</sup> However, other studies indicate that the features are more likely to be characteristic of the bulk.<sup>1</sup> We note that the identification of surface states is difficult for this material. One of the crucial tests for a surface state is that the feature should be nondispersive in the direction perpendicular to the surface. This test is meaningless here because the bulk material under study is also highly two dimensional. Gas adsorption studies using  $\text{O}_2$  and Ar do not show any preferential attenuation of the 1-eV peak.<sup>1</sup> The fact that the 1-eV peak is observed consistently in many samples with different cleaves also suggests that this feature cannot be of surface origin, since different cleaves are likely to expose different layers of the crystal structure on the topmost layer.<sup>4</sup> The appearance of the feature through much of the Brillouin zone also indicates that it is of bulk origin, since a surface state can only exist in certain parts of the zone where there exists a bulk band gap.

Shown in Figs. 2(a)–2(d) are EDC's measured on samples with oxygen stoichiometries  $x=6.5$ , 6.4, 6.3, and 6.2, respectively. The corresponding  $k$  points for each set of spectra are approximately the same as in Fig. 1. It can be seen that, for oxygen stoichiometries  $x=6.5$  and 6.4 [Figs. 3(a) and 3(b)], spectral features have intensities comparable to those in Fig. 1 ( $x=6.9$ ) and similar dispersions. When the oxygen stoichiometry is reduced to  $x=6.3$  where the sample is barely insulating (i.e., the  $a$ - $b$

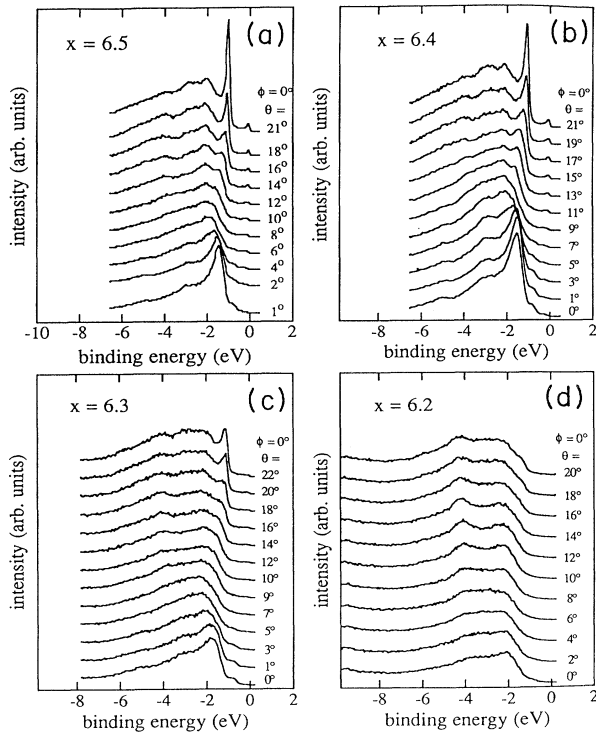


FIG. 2. EDC's measured on  $\text{YBa}_2\text{Cu}_3\text{O}_x$  samples with oxygen stoichiometry (a)  $x=6.5$ , (b)  $x=6.4$ , (c)  $x=6.3$ , and (d)  $x=6.2$ , for  $k$  points along  $\Gamma$ - $X$  ( $Y$ ).  $h\nu=24$  eV were used for all spectra. The corresponding  $k$  points for each set of spectra are (nearly) the same as those shown in the inset of Fig. 1.

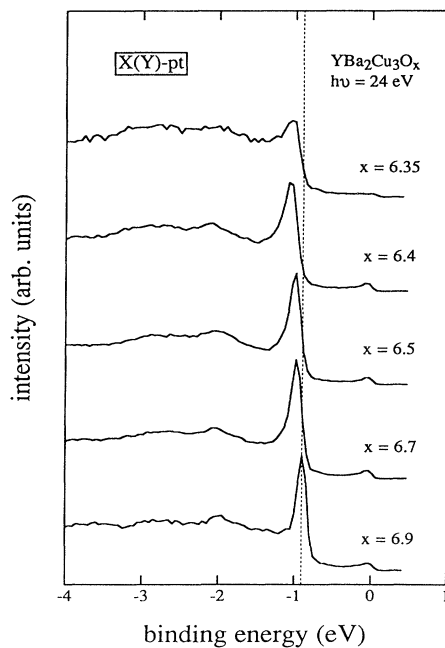


FIG. 3. EDC's measured on a series of samples with different oxygen stoichiometries which are marked along each curve. All spectra are taken at the  $X$  ( $Y$ ) point(s).

plane resistivity shows a semiconducting upturn at low temperature), spectra start to show dramatic change. Notably, the 1-eV peak at the  $X$  ( $Y$ ) point(s) is significantly attenuated. The 1-eV peak is no longer discernible at  $x=6.2$  where the sample is even more insulating. For this sample, nearly all sharp features are diminished and the spectra appear mostly featureless. Clearly, the spectral behavior as a function of oxygen stoichiometry is distinctly different in the metallic and in the insulating regimes. In the following, we shall examine and discuss the behavior in each regime in more detail.

Although the general appearances of the valence-band spectra are similar when oxygen stoichiometry is varied between  $x=6.9$  and  $6.4$ , there do exist subtle yet finite and systematic changes. Shown in Fig. 3 is a set of EDC's measured at the same  $k$  point [the  $X$  ( $Y$ ) point(s)] for a series of samples with different oxygen stoichiometries. The vertical dashed line indicates the binding energy of the 1-eV peak for the fully oxygenated ( $x=6.9$ ) sample. It can be seen that, as oxygen is removed, the 1-eV peak shifts nearly monotonically toward higher binding energies. Plotted in Fig. 4 are the measured 1-eV peak binding energies as a function of oxygen stoichiometry. The error bar ( $\pm 0.02$  eV) is a conservative estimate of the uncertainty in the binding energy determinations. The amount of shift relative to  $x=6.9$  is 0.08 eV for  $x=6.7$ , 0.07 eV for  $x=6.6$ , 0.08 eV for  $x=6.5$ , 0.13 eV for  $x=6.4$ , 0.15 eV for  $x=6.35$ , and 0.20 eV for  $x=6.3$ . The position of the 1-eV peak cannot be tracked below  $x=6.3$  since the peak is no longer well defined.

In these experiments, the position of the Fermi level, our energy reference for all samples, is taken as the midpoint of the rising edge of the EDC measured from a clean platinum foil which is in electrical contact with the YBCO samples. The validity of this procedure is based on the simple fact that equilibrium requires that the Fermi levels of electrically connected materials be the same. If we consider the distinct 1-eV peak as an energy reference and force this peak to line up for samples with different oxygen stoichiometries, then the observed shifts can be interpreted as an increase of the Fermi level for decreasing oxygen content. This trend is consistent with

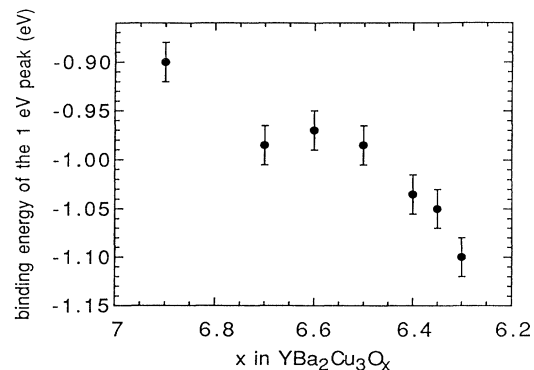


FIG. 4. Measured binding energies of the 1-eV peak vs oxygen stoichiometry.

the hole doping picture. Based on the calculated density of states obtained using the self-consistent linearized augmented plane-wave method and assuming rigid band filling, Krakauer, Pickett, and Cohen<sup>19</sup> estimated the Fermi-level difference between  $x=6.7$  and  $6.9$  to be  $0.056$  eV. This value is slightly smaller than the observed shift which is  $0.08$  eV. The observed amount of shift might indicate that the actual density of states is slightly lower than the calculated value.

We note that the trend of the 1-eV peak binding energy as a function of oxygen stoichiometry (Fig. 4) has some similarity to that of the superconducting transition temperature  $T_c$ . In particular, note that the binding energy of the 1-eV peak displays a plateau-like behavior near  $x=6.6$ , mimicking the lower "plateau" in the  $T_c$  vs oxygen stoichiometry curve. If the observed energy shifts of the 1-eV peak can be attributed to changes in carrier concentration as discussed above, the similarity suggests that  $T_c$  and carrier concentration are directly related. Correlation between  $T_c$  and carrier concentration has, of course, been noted in many previous studies. Further, it is commonly believed that the "plateau" in  $T_c$  near  $x=6.5$  is due to oxygen vacancy ordering in the Cu-O chains.<sup>14</sup> A simple model calculation,<sup>20</sup> incorporating the assumption that two coordinated Cu atoms (chain Cu's) are monovalent, indicates that carrier concentration varies with oxygen ordering.

We now turn our attention to the insulating regime. Shown in Fig. 5 is a direct comparison of three EDC's taken at the same  $k$  point [the  $X(Y)$  point(s)] on samples with oxygen stoichiometries  $x=6.4$ ,  $6.3$ , and  $6.2$ , respectively. The intensities are normalized to the average emission intensities above the Fermi level.<sup>3</sup> It can be seen that the intensity of the 1-eV peak is significantly attenuated when oxygen stoichiometry is reduced from  $x=6.4$  to  $6.3$ . The features at higher binding energies also become less well defined. Note that the difference in oxygen content between these two samples is relatively small. However, one sample is a superconductor ( $T_c=33$  K) and the other is an insulator (semiconductor). Evi-

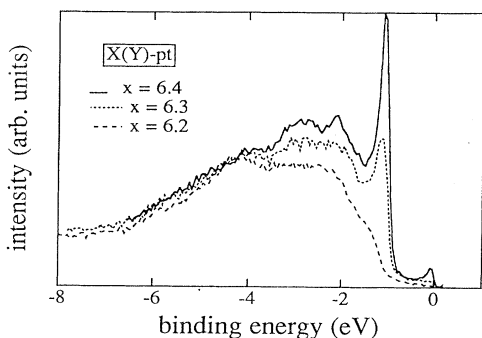


FIG. 5. Comparison of three EDC's measured on samples with oxygen stoichiometries  $x=6.4$  (solid line),  $6.3$  (short dashed line), and  $6.2$  (long dashed line), respectively. The corresponding  $k$  point is the  $X(Y)$  point(s) for all spectra.  $h\nu=24$  eV were used for all spectra. The spectral intensities are normalized to the average emission intensities above the Fermi level.<sup>3</sup>

dently, dramatic spectral changes occur at the onset of the metal-insulator transition. At  $x=6.2$ , the 1-eV peak is diminished to merely a shoulder.

Figure 5 also shows that the spectral intensity at the Fermi level is strongly attenuated when the material becomes insulating. In our previous papers,<sup>2,3</sup> it was shown that, for the fast dispersing bands near  $E_F$  along the zone diagonal  $\Gamma$ - $S$ , both the peak intensities and the Fermi surfaces they define (the places where the bands cross the Fermi level), are nearly invariant (i.e., independent of oxygen stoichiometry), in the metallic regime. However, the intensity at  $E_F$  decreases abruptly at the onset of the metal-insulator transition. The flat bands observed at  $E_F$  along the zone edge  $\Gamma$ - $X(Y)$  have similar behavior. To illustrate, we show, in Fig. 6, EDC's along  $\Gamma$ - $X(Y)$ - $\Gamma'$  for a narrow energy window near  $E_F$  measured on samples with oxygen stoichiometries (a)  $x=6.5$  and (b)  $x=6.3$ . At  $x=6.5$ , when  $k$  is scanned from  $\Gamma$  toward  $Y$ , a peak disperses from below  $E_F$  to near  $E_F$ , and stays very close to  $E_F$  for an extended region, then disperses back below  $E_F$  as  $\Gamma'$  is approached. The peak dispersion and peak intensities are similar to those observed in a fully oxygenated sample.<sup>16</sup> This flat band is interpreted as evidence for an extended van Hove singularity (VHS).<sup>21</sup> It was suggested that the VHS might play a significant role in enhancing  $T_c$ .<sup>22</sup> As can be seen in Fig. 6, most of the peak intensity is lost when  $x=6.3$ . Only a hint of the underlying dispersion can be seen.

We note that the spectral behavior at  $E_F$  is not quite consistent with a rigid band picture. In the rigid band

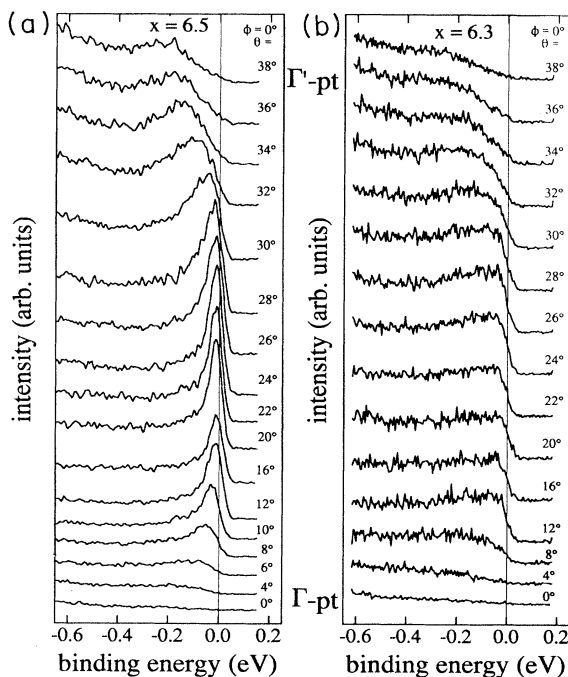


FIG. 6. EDC's for a narrow energy window near  $E_F$  measured on samples with oxygen stoichiometry (a)  $x=6.5$  and (b)  $x=6.3$ .  $h\nu=28$  eV were used. The corresponding  $k$  points are along  $\Gamma$ - $Y$ - $\Gamma'$ .

picture, one would expect to see the peak (VHS) at  $E_F$  shift toward higher binding energies, just as the 1-eV peak does, when oxygen stoichiometry is reduced. What is observed, however, is that the peak (VHS) remains very close to the Fermi level when oxygen stoichiometry is varied. The shift, if any, is less than 10 meV within the metallic regime. When oxygen stoichiometry is sufficiently reduced so that the material becomes insulating, only the intensity drops. Clearly, the doping mechanism is more complicated than the simple rigid band picture suggests. Abrikosov<sup>23</sup> has argued that the Fermi energy with respect to the VHS peak will be expected to increase, to approximately 30 meV, as  $T_c$  declines to 40 K with composition (see Fig. 4 in Ref. 23). It would appear, however, that the observed shift in oxygen-deficient metallic YBCO is less than this predicted value. The fact that the VHS is observed very close to  $E_F$  in the  $x=6.5$  sample ( $T_c=50$  K) suggests that the link between VHS and  $T_c$  either is not simple or does not exist.  $T_c$  might be a very sensitive function of the details of the VHS, such as its extent and energy position, as suggested by King *et al.*<sup>24</sup> More detailed studies are under way.<sup>25</sup>

Could the intense spectral features at  $E_F$  be of nonintrinsic origin? It has been suggested that they might originate from spatially localized impurities in the samples. This is unlikely since spatially localized impurity states would be  $k$  independent in reciprocal space. These features are observed to disperse in the Brillouin zone. Furthermore, the features are very robust in that they appear consistently in many different samples, which also suggests that they are not of impurity origin. It was also suggested that these states appear at the Fermi level as a result of a surface Madelung potential that is different from the bulk; in other words, these states are surface states. We think that this is unlikely for the same reasons presented above in the discussion of the 1-eV peak.

It is not clear why distinct spectral features, both at  $E_F$  and 1 eV binding energy, disappear when the material becomes insulating. We caution that the loss of the spectral intensity observed here should not be interpreted as a reduction of the density of states, because only states in a small momentum window are sampled in the angle-resolved photoemission experiments. In the metallic regime, the intense features at  $E_F$  can be interpreted as quasiparticle peaks. A reasonable explanation for the loss of these features in the insulating regime is that the quasiparticle weight is diminished as a result of strong electron-electron correlation.

It is possible that the 1-eV peak is attenuated as a re-

sult of disorder in the severely oxygen-deficient samples. For oxygen-deficient samples, some degree of disorder exists in the chain basal plane due to oxygen vacancies. At  $x=6.5$ , the oxygen vacancies have a strong tendency to order into alternately filled and empty chains to form the Ortho II structure.<sup>14</sup> At different stoichiometries, other ordered structures also exist (e.g., Ortho III at  $x=6.67$ ). Possibly, in the metallic region, with  $x>6.4$ , oxygen vacancies may be only moderately disordered, and consequently have little effect on the 1-eV peak. For severely oxygen-deficient samples, such as those with  $x=6.3$  and 6.2, the degree of disorder could be more severe. It is conceivable that the 1-eV peak, whose dispersing behavior shows a clear connection with the crystallographic periodicity, might be destroyed by the increased disorder. However, oxygen ordering clearly occurs with  $x<6.4$ ,<sup>26,27</sup> though possibly with a smaller tendency to form linear chains of vacancies. The rather abrupt loss of the 1-eV feature for  $x<6.4$ , near the metal-insulator transition, and the observation of order in extremely oxygen-deficient samples, suggests that the existence of metallic conductivity is a more important condition than the state of order for observation of the feature.

In summary, the ARPES spectra show very different behavior as a function of doping in the metallic and in the insulating regimes. The distinct 1-eV peak at the  $X(Y)$  point(s) shifts monotonically toward higher binding energies as oxygen stoichiometry is reduced from  $x=6.9$  to 6.3. The direction and the magnitude of the shift are consistent with a simple rigid-band filling picture. However, it is shown that such a picture is not consistent with the observed spectral behavior at  $E_F$ . Spectral features at  $E_F$  remain at nearly the same position as oxygen stoichiometry is varied. Distinct spectral features, both at 1 eV below  $E_F$  and at  $E_F$ , are significantly attenuated when the material becomes insulating. We suggest that the attenuation of the spectral features at  $E_F$  is a consequence of strong electron-electron correlation in the insulating samples.

Work at Argonne National Laboratory is supported by the U.S. DOE under Contract No. W-31-109-ENG-38 (B.W.V., A.P.P., and P.J.K.) and by the NSF, Science and Technology Center for Superconductivity, under Contract No. DMR 91-20000 (R.L. and C.G.). Ames Laboratory is operated for the U.S. DOE by Iowa State University under Contract No. W-7405-ENG-82. The Synchrotron Radiation Center is supported by the NSF under Contract No. DMR 8601349.

<sup>1</sup>J. G. Tobin, C. G. Olson, C. Gu, J. Z. Liu, F. R. Solal, M. J. Fluss, R. H. Howell, J. C. O'Brien, H. B. Radousky, and P. A. Sterne, *Phys. Rev. B* **45**, 5563 (1992).

<sup>2</sup>R. Liu, B. W. Veal, A. P. Paulikas, J. W. Downey, P. J. Kostic, S. Fleshler, U. Welp, C. G. Olson, X. Wu, A. J. Arko, and J. J. Joyce, *Phys. Rev. B* **46**, 11 056 (1992).

<sup>3</sup>R. Liu, B. W. Veal, A. P. Paulikas, J. W. Downey, H. Shi, C. G. Olson, C. Gu, A. J. Arko, and J. J. Joyce, *Phys. Rev. B* **45**, 5614 (1992).

<sup>4</sup>B. W. Veal, R. Liu, A. P. Paulikas, D. D. Koelling, H. Shi, J. W. Downey, C. G. Olson, A. J. Arko, J. J. Joyce, and R. Blyth, *Surf. Sci. Rep.* **19**, 121 (1993); B. W. Veal and C. Gu, *J.*

- Electron Spectrosc. Relat. Phenom. **66**, 321 (1994).
- <sup>5</sup>G. Mante, R. Claessen, A. Huss, R. Manzke, M. Skibowski, Th. Wolf, M. Knupfer, and J. Fink, Phys. Rev. B **44**, 9500 (1991).
- <sup>6</sup>C. G. Olson, R. Liu, D. W. Lynch, R. S. List, A. J. Arko, B. W. Veal, Y. C. Chang, P. Z. Jiang, and A. P. Paulikas, Phys. Rev. B **42**, 381 (1990).
- <sup>7</sup>D. S. Dessau, Z. X. Shen, D. M. King, D. S. Marshall, L. W. Lombardo, P. H. Dickinson, A. G. Loeser, J. Dicarolo, C. H. Park, A. Kapitulnik, and W. E. Spicer, Phys. Rev. Lett. **71**, 2781 (1993).
- <sup>8</sup>P. W. Anderson, Phys. Scr. **T42**, 11 (1992).
- <sup>9</sup>J. W. Allen, C. G. Olson, M. B. Maple, J. S. Kang, L. Z. Liu, J. H. Park, R. O. Anderson, W. P. Ellis, J. T. Market, Y. Dalichaouch, and R. Liu, Phys. Rev. Lett. **64**, 595 (1990).
- <sup>10</sup>Z. X. Shen, D. S. Dessau, B. O. Wells, C. G. Olson, D. B. Mitzi, L. Lombardo, R. S. List, and A. J. Arko, Phys. Rev. B **44**, 12 098 (1991).
- <sup>11</sup>H. Matsuyama, T. Takahashi, H. Katayama-Yoshida, T. Kashiwakura, Y. Okabe, S. Sato, N. Kosugi, A. Yagishita, K. Tanaka, H. Fujimoto, and H. Inokuchi, Physica C **160**, 567 (1989).
- <sup>12</sup>P. Almeras *et al.*, Solid State Commun. **91**, 535 (1994).
- <sup>13</sup>D. L. Kaiser, F. Holtzberg, B. A. Scott, and T. R. McGuire, Appl. Phys. Lett. **51**, 1040 (1987); L. P. Schneemeyer, J. V. Waszczak, T. Siegrist, R. B. van Dover, L. W. Rupp, B. Batlogg, R. J. Cava, and D. W. Murphy, Nature **328**, 601 (1987); J. P. Rice, B. G. Pazol, D. M. Ginsberg, T. J. Moran, and M. B. Weissman, J. Low Temp. Phys. **72**, 345 (1988).
- <sup>14</sup>B. W. Veal, A. P. Paulikas, H. You, H. Shi, Y. Fang, and J. W. Downey, Phys. Rev. B **42**, 4770 (1990); **42**, 6305 (1990); J. D. Jorgensen, S. Pei, P. Lightfoot, H. Shi, A. P. Paulikas, and B. W. Veal, Physica C **167**, 571 (1990); H. Claus, S. Yang, A. P. Paulikas, J. W. Downey, and B. W. Veal, *ibid.* **171**, 205 (1990).
- <sup>15</sup>C. G. Olson, Nucl. Instrum. Methods Phys. Res. Sect. A **266**, 205 (1988).
- <sup>16</sup>J. G. Tobin and C. G. Olson *et al.* (unpublished).
- <sup>17</sup>R. Claessen, G. Mante, A. Huss, R. Manske, M. Skibowski, Th. Wolf, and J. Fink, Phys. Rev. B **44**, 2399 (1991).
- <sup>18</sup>C. Calandra, F. Manghi, and T. Minerva, Phys. Rev. B **46**, 3600 (1992).
- <sup>19</sup>H. Krakauer, W. E. Pickett, and R. E. Cohen, J. Supercond. **1**, 111 (1988).
- <sup>20</sup>B. W. Veal and A. P. Paulikas, Physica C **184**, 321 (1991).
- <sup>21</sup>K. Gofron, J. C. Campuzano, H. Ding, C. Gu, R. Liu, B. Dabrowski, B. W. Veal, and G. Jennings, J. Phys. Chem. Solids **54**, 1193 (1993); K. Gofron, J. C. Campuzano, A. A. Abrikosov, M. Lindroos, A. Bansil, H. Ding, D. Koelling, and B. Dabrowski, Phys. Rev. Lett. **73**, 3302 (1994).
- <sup>22</sup>A. A. Abrikosov, J. C. Campuzano, and K. Gofron, Physica C **214**, 73 (1993).
- <sup>23</sup>A. A. Abrikosov, Physica C **233**, 102 (1994).
- <sup>24</sup>D. M. King, Z. X. Shen, D. S. Dessau, D. S. Marshall, C. H. Park, W. E. Spicer, J. L. Peng, Z. Y. Li, and R. L. Greene, Phys. Rev. Lett. **73**, 3298 (1994).
- <sup>25</sup>C. Gu *et al.* (unpublished).
- <sup>26</sup>H. Shaked, J. D. Jorgensen, B. A. Hunter, R. L. Hitterman, A. P. Paulikas, and B. W. Veal, Phys. Rev. B **51**, 547 (1995).
- <sup>27</sup>R. Sonntag, D. Hohlwein, T. Bruckel, and G. Collin, Phys. Rev. Lett. **66**, 1497 (1991).